

# Molecular Strategies for Morphology Control in Semiconducting Polymers for Optoelectronics

Aiman Rahmanudin and Kevin Sivula\*

**Abstract:** Solution-processable semiconducting polymers have been explored over the last decades for their potential applications in inexpensively fabricated transistors, diodes and photovoltaic cells. However, a remaining challenge in the field is to control the solid-state self-assembly of polymer chains in thin films devices, as the aspects of (semi)crystallinity, grain boundaries, and chain entanglement can drastically affect intra- and intermolecular charge transport/transfer and thus device performance. In this short review we examine how the aspects of molecular weight and chain rigidity affect solid-state self-assembly and highlight molecular engineering strategies to tune thin film morphology. Side chain engineering, flexibly linking conjugation segments, and block co-polymer strategies are specifically discussed with respect to their effect on field effect charge carrier mobility in transistors and power conversion efficiency in solar cells. Example systems are taken from recent literature including work from our laboratories to illustrate the potential of molecular engineering semiconducting polymers.

**Keywords:** Conjugated polymers · Photovoltaics · Semicrystalline · Solution-processing · Transistors

## 1. Introduction

Semiconducting polymers, which generally possess a  $\pi$ -conjugated backbone to give HOMO-LUMO gaps in the 1–3 eV range, have attracted significant attention over the last decades from both academic and industrial laboratories due to a wealth of potential applications from solution-processed thin-film electronics to the roll-to-roll fabrication of light-emitting diodes and photovoltaic cells.<sup>[1]</sup> The tools of organic chemistry have been extensively applied to manipulate polymer architecture and have led to a vast library of semiconducting polymers with a variety of functionalities.<sup>[2]</sup> While tuning the band-gap, electron affinity and processability of semiconducting polymers have been well developed, critical challenges involving understanding and controlling the relationships between molecular structure, the solid-state self-assembly, and the resulting optoelectronic properties remain to be addressed in order to fully realize the potential of these materials.<sup>[3]</sup>

This is exemplified by the apparent discord between the maximum predicted charge carrier (hole) mobility,  $\mu_h$ , using density functional theory (DFT) – which does not typically consider the macroscopic thin-film morphological structure<sup>[4]</sup> – to experimentally measured field-effect  $\mu_h$  in organic-thin-film-transistors (OTFTs). For prototypical thiophene-based polymers such as poly(3-hexylthiophene), P3HT, and poly-2,5-bis[3-alkylthiophen-2-ylthiono(3,2-*b*)thiophene], PBTTT, DFT gives  $\mu_h$  as high as 31 and 15 cm<sup>2</sup> V<sup>-1</sup> s<sup>-1</sup>, respectively, but OFETs show  $\mu_h$  only up to 0.1 and 1.0 cm<sup>2</sup> V<sup>-1</sup> s<sup>-1</sup>.<sup>[5]</sup> This discrepancy suggests that substantial improvements in performance remain attainable. In this short review we will give an overview of the nature of the complexity behind the links between structure, morphology, and function in solution-processed semiconducting polymers and highlight current strategies to further advance the field toward engineering the self-assembly of these promising materials.

## 2. Influence of Molecular Weight and Dispersity

Of fundamental importance for any polymer are the aspects of molecular weight and dispersity. As the prototypical P3HT can be readily prepared *via* quasi-living coupling reactions (*e.g.* Grignard metathesis)<sup>[6]</sup> giving good control over the molecular weight and dispersity,  $\mathcal{D}$ , the influence of chain length on thin film morphology and performance has been well

established.<sup>[7]</sup> Because the P3HT backbone (see structure in Scheme 1) has significant conformational rigidity (compared to traditional coil-type polymers like polystyrene or polymethylmethacrylate) and can interact *via*  $\pi$ -stacking, a strong influence of the number-average molecular weight,  $M_n$ , on the resulting thin film morphology and performance is observed. With increasing molecular weight (chain length) of the polymer, the solid-state self-assembly transits from a highly ordered extended chain conformation, where chain rigidity and  $\pi$ -stacking dominate the self-assembly, to a folded structure of alternating crystalline lamellae and amorphous disordered zones where eventually chain entanglement occurs (Fig. 1a.).<sup>[8]</sup> Interestingly, the highly-ordered structures found in low molecular weight P3HT result in poor charge carrier mobility in macroscopic thin films as charge trapping sites at grain boundaries limit the transport of carrier over long distances. Thus, molecular weights over the critical entanglement molecular weight,<sup>[9]</sup>  $M_c$ , of *ca.* 35 kg mol<sup>-1</sup> are typically sought for good performance as increasing  $M_n$  over this value (up to 150 kg mol<sup>-1</sup>) does not increase the charge transport performance in thin film transistors.

The control over molecular weight in the poly(3-alkylthiophenes) is exceptional as most modern conjugated polymers cannot be prepared *via* quasi-living approaches. Rather, the majority are prepared *via* carbon-carbon cross-coupling polycondensation reactions (*e.g.* Stille or Suzuki couplings) that lead to relatively low number average molecular weights ( $M_n < 100$

\*Correspondence: Prof. Dr. K. Sivula  
Ecole Polytechnique Fédérale de Lausanne (EPFL)  
Institut des Sciences et Ingénierie Chimiques  
Laboratory for Molecular Engineering of  
Optoelectronic Nanomaterials (LIMNO)  
EPFL SB ISIC LIMNO, Station 6  
CH-1015 Lausanne  
E-mail: kevin.sivula@epfl.ch

kg mol<sup>-1</sup>) and dispersity,  $\mathcal{D}$ , approaching 2. This complicates the study of the effects of molecular weight and dispersity on the thin film morphology and performance. Recently, our group has used preparatory size exclusion chromatography to isolate fractions of PBTTT (see Scheme 1) from 5.8 to 150 kg mol<sup>-1</sup> with  $\mathcal{D} = 1.1$ –1.4 for study in OTFTs.<sup>[10]</sup> This study was motivated by the observations that PBTTT uniquely self-assembles into 2D lamella (after thermal annealing at 180 °C) due to its rigid polymer backbone that promotes  $\pi$ -stacking together with linear and sparse solubilizing alkyl chains that interdigitate.<sup>[11]</sup> We found the microstructure and crystallinity of the various  $M_n$  fractions of PBTTT to show three distinct morphological behaviors: fiber formation (*ca.* 5–20 kg mol<sup>-1</sup>), terraces due to 2D lamella formation (20–50 kg mol<sup>-1</sup>), and a rough entangled morphology (60–150 kg mol<sup>-1</sup>), (Fig. 1b). Interestingly, the more rigid backbone structure in PBTTT compared to P3HT leads to an increase in  $M_c$  to *ca.* 60 kg mol<sup>-1</sup>. The corresponding  $\mu_h$  measured for the different molecular weight fractions reflected a rapid improvement in performance from low molecular weights with increasing chain length, with the highest mobility measured for polymers with a 2D terraced morphology, which eventually decreased towards higher molecular weights of the polymer greater than  $M_c$ . This decrease at high  $M_n$  is distinct from P3HT (where  $\mu_h$  remains constant for  $M_n > M_c$ ) and suggests that the 2D self-assembly of PBTTT in the lamella arrangement improves intermolecular charge transport even though this self-assembly was found to be only paracrystalline.<sup>[12]</sup> With regards to molecular weight dispersity, upon blending low amounts of high molecular weight (5%wt) with low molecular weight PBTTT, no terrace formation was observed, and  $\mu_h$  remained below the best values with the terrace-forming medium molecular weight PBTTT, reinforcing the notion that the polymer's tertiary structure is critical to macroscopic performance. In addition, studies of the molecular weight dependence of other semicrystalline  $\pi$ -conjugated polymers, show a dependence of charge carrier mobility on  $M_n$  similar of that to P3HT.<sup>[13]</sup>

### 3. Side Chain Engineering

The different behavior between P3HT and PBTTT discussed above is, to some extent, caused by a dissimilar self-assembly of the solubilizing alkyl side chains. Indeed, engineering the structure of the solubilizing side chains has been extensively investigated as an approach to tuning the self-assembly of the conjugated

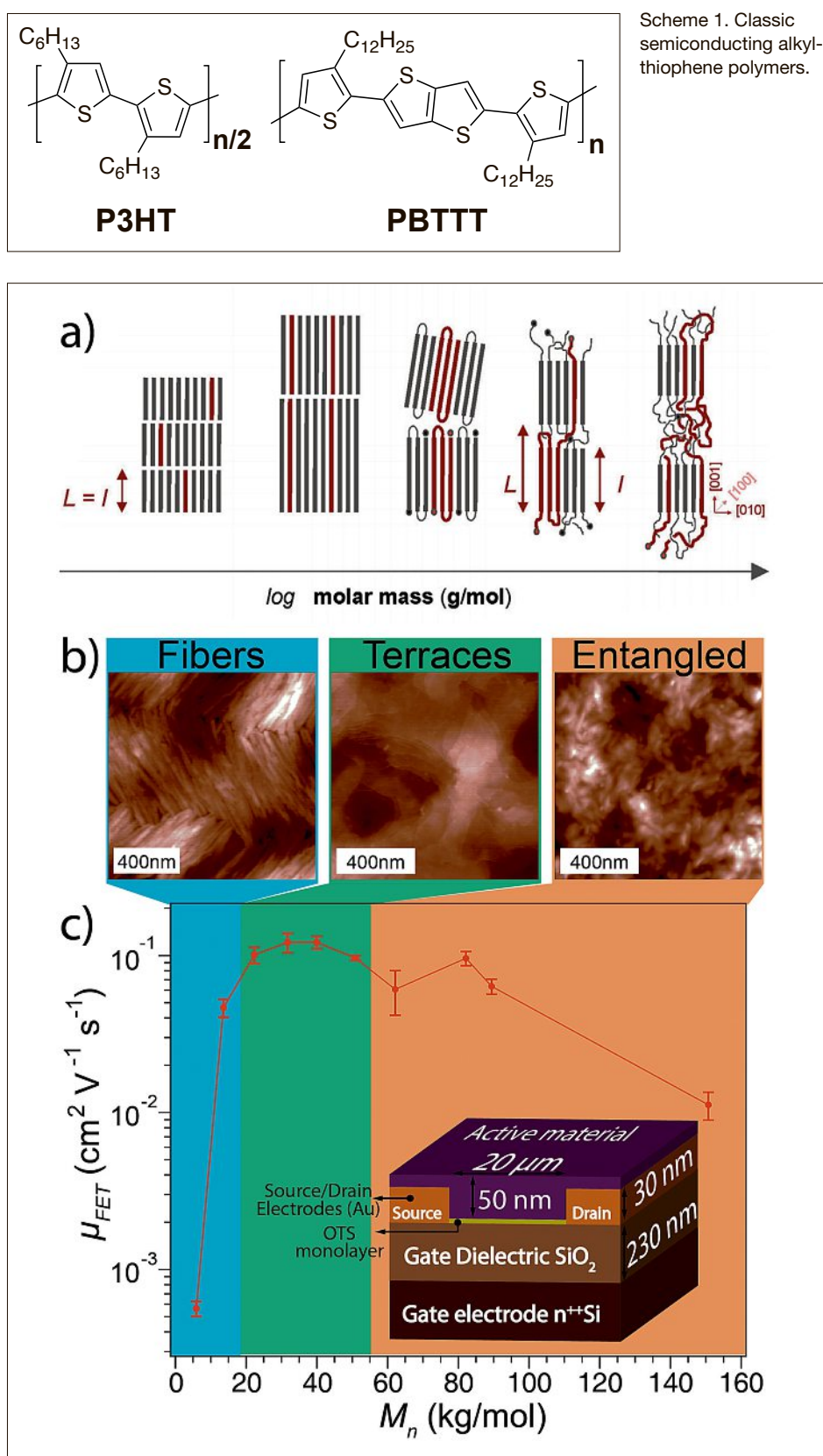


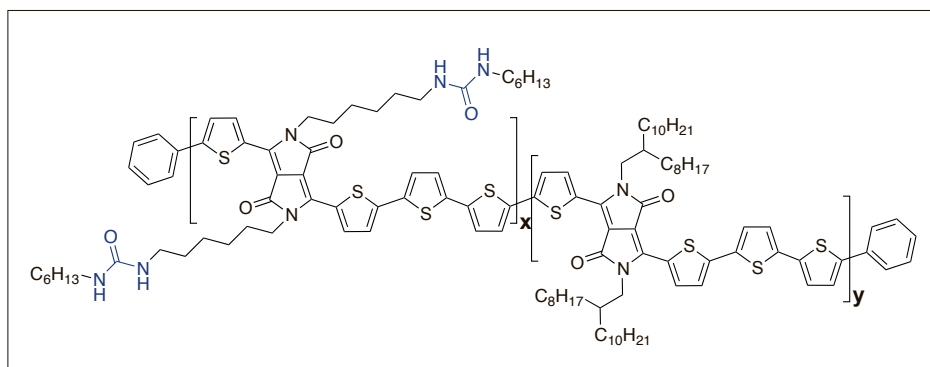
Fig. 1. (a) Schematic illustration of the evolution of the molecular arrangement of a (semi-)flexible polymer such as P3HT in the solid state. The length of the extended chain,  $l$  (between grain boundary or entanglements) and the long period  $L$ , *i.e.*, the total thickness of the crystalline and amorphous region, are defined as indicated in red. Reproduced from ref. [9], © 2013 Elsevier used with permission. (b) Tapping-mode atomic force microscopy (AFM) images of the surface morphology of PBTTT films with different molecular weight (5.8 kg/mol, 40.0 kg/mol and 89.7 kg/mol respectively). (c) Average extracted (saturation regime) field-effect charge carrier (hole) mobility,  $\mu_{FET}$ , of annealed (180 °C, 10 min) PBTTT fractions as a function of number average molecular weight,  $M_n$ . Error bars corresponding to one standard deviation on multiple devices are also shown, and the inset shows a schematic of the OTFT device used. (b) and (c) are adapted from ref. [10], © 2014 American Chemical Society.

polymer.<sup>[14]</sup> Moreover, modifying the self-assembly can be accomplished without significantly altering the molecular structure of the core backbone by including functional groups at the solubilizing chain ends.<sup>[15]</sup> As these functional moieties are positioned away from the conjugated backbones, they typically do not directly affect the HOMO-LUMO gap of the polymer. However, they can have a large effect on the thin morphology, solubility (e.g. by including ionic<sup>[16]</sup> or oligoether<sup>[17]</sup> side chains), or give added functionalities (e.g. cross linking abilities<sup>[18]</sup> or cleavable groups<sup>[19]</sup>).

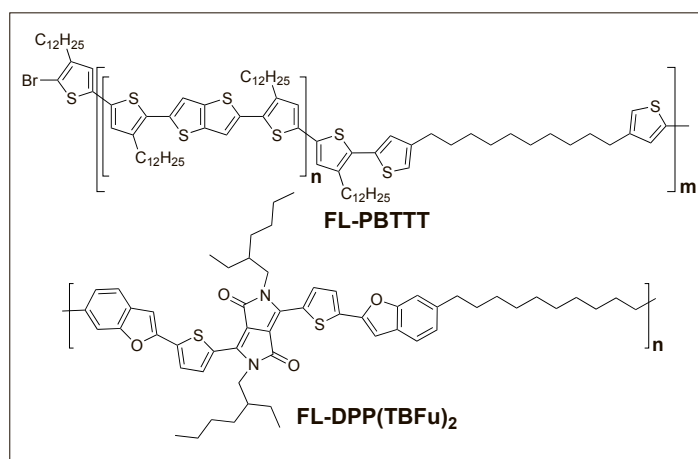
One recent example of the power of side chain engineering is from Yao *et al.* who employed a series of diketopyrrolopyrrole (DPP)–quaterthiophene conjugated polymers with varying degrees of a urea-containing alkyl chain vs a standard (branched) alkyl chain (structure in Scheme 2).<sup>[20]</sup> The incorporation of urea groups in the alkyl side chains was found to have an interesting effect on the lamellar packing order of the alkyl chains due to hydrogen bonding interactions between urea groups. A polymer with an optimized incorporation of urea groups (x:y in Scheme 2 equal to 1:10) was found to exhibit a OTFT  $\mu_h$  of up to  $13.1 \text{ cm}^2 \text{ V}^{-1} \text{ s}^{-1}$  after thermal annealing at  $100 \text{ }^\circ\text{C}$ . It is noted that this is among the highest  $\mu_h$  reported for conjugated polymers to date. However, overall since the self-assembly of a typical polymer semiconductor is dominated by  $\pi$ - $\pi$  interactions, side chain engineering approaches offer relatively limited control and despite the functional group being isolated from the conjugated backbone, these groups can potentially lead to the introduction of electronic trapping states.<sup>[14]</sup>

#### 4. Conjugation Break Spacer (Flexible Linker) Approach

Another interesting method to control the supramolecular assembly of semiconducting polymers without altering the semiconducting core has been suggested *via* the covalent tethering of conjugated segments with flexible non-conjugated chains.<sup>[21]</sup> Employing these ‘flexible linkers’ – which break continuous backbone conjugation – has recently shown promising effects by easing chain rigidity, increasing processability, and offering unique self-assembly motifs.<sup>[22]</sup> Melt-processing semiconducting polymers while still obtaining good device performance has even been demonstrated with this approach.<sup>[22i]</sup> Our group has used the conjugation break spacer (or flexible linker) approach to investigate the relationship between self-assembly and charge transport in PBTTT.<sup>[22d]</sup> We synthesized short PBTTT segments joining them



Scheme 2. A diketopyrrolopyrrole-quaterthiophene conjugated (random) co-polymer with varying degrees of a urea-containing alkyl chain vs a branched alkyl chain.



Scheme 3. Flexibly-linked semiconducting polymers.

into the flexibly-linked FL-PBTTT structure shown in Scheme 3 (with  $n = 10$ – $12$ ,  $m = 4$ – $5$ ). The FL-PBTTT was found to exhibit distinct thin-film morphologies (from rod-like fibrils, to 2D terraces, see Fig. 2) by just changing the processing conditions and without changing the molecular weight or the length of the conjugated segments. In OTFT devices changing the film morphology gave rise to an improvement

of the charge carrier mobility from fibril-type ( $0.01 \text{ cm}^2 \text{ V}^{-1} \text{ s}^{-1}$ ) to terrace morphologies ( $0.04 \text{ cm}^2 \text{ V}^{-1} \text{ s}^{-1}$ ) while actually decreasing the overall crystallinity of the film as indicated by the intensity of the X-ray diffraction (see Fig. 2). When compared to a fully-conjugated, high molecular weight PBTTT sample, our results suggested that the high  $\mu_h$  of PBTTT is not solely due to improved intramolecular transport

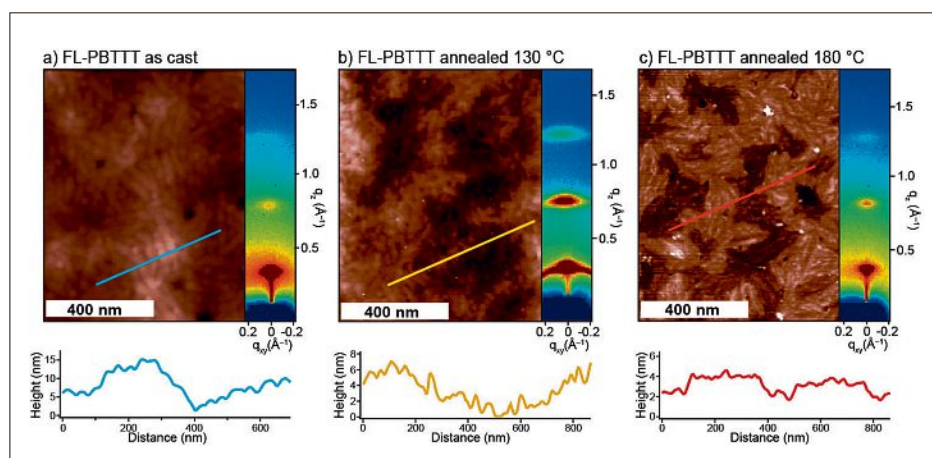


Fig. 2. Tapping mode AFM topography of: a) FL-PBTTT as cast from *o*-dichlorobenzene  $20 \text{ mg mL}^{-1}$ , b) FL-PBTTT after annealing at  $130 \text{ }^\circ\text{C}$ , and c) after annealing at  $180 \text{ }^\circ\text{C}$ . The topographical profile along the indicated diagonal line in each case is shown below. The right side of each panel shows the 2D grazing -incidence X-ray diffraction plots of the same films with the vertical direction corresponding to the out-of-plane scattering vector,  $q_z$ , and the horizontal direction corresponding to  $q_{xy}$ . Red areas represent the highest scattering intensity while blue represent the lowest. Adapted from ref. [22d], © The Royal Society of Chemistry 2014.

(thought to be caused by increasing the linearity of the chains<sup>[23]</sup>) but that the 2D charge-transport network afforded by self-assembly contributes significantly to the observed high charge carrier mobility.

In contrast it should be noted that recent high-performance polymers with increasingly sophisticated monomeric moieties such as naphthalenediimides,<sup>[24]</sup> diketopyrrolopyrrole,<sup>[25]</sup> and carbazoles<sup>[26]</sup> do not show long range crystalline order like P3HT and PBTTT but exhibit superior  $\mu_h$  over  $1 \text{ cm}^2 \text{ V}^{-1} \text{ s}^{-1}$ .<sup>[12]</sup> Despite their seemingly disordered morphology, these polymers do, however, exhibit solid-state aggregation consistent with improved intramolecular associations (indicative from resolvable vibronic progression near the absorption edge, *i.e.* red shifting, in their optical absorption spectra).<sup>[27]</sup> Thus these recent results point to the conclusion that short-range ordering of stacked aggregates seems sufficient for efficient charge transport, so long as the aggregates are sufficiently interconnected.<sup>[28]</sup> Therefore, based on the discussion above, it has been concluded in the field that a unifying requirement for efficient charge mobility is not to induce high crystallinity in the semiconducting polymer film, but to improve the interconnectedness between aggregated domains, and reduce the amount of disorder within conjugated segments to facilitate intra- and intermolecular charge transport on the macroscopic level.

The flexible linker strategy is very useful in this regard to improve connectivity in thin films of small-molecule semiconductors. Indeed, while solution-processable small molecule (non-polymeric) semiconductors have purported advantages over polymer semiconductors including synthetic simplicity and the ability to eliminate batch-to-batch variations,<sup>[29]</sup> they typically suffer from similar drawbacks as low molecular weight  $\pi$ -conjugated polymers (*i.e.* a strong tendency to self-assemble into crystalline domains which results in film

dewetting, unpredictable crystallite sizes, and grain boundaries) that confound the morphological control and charge transport in devices fabricated from these materials. Recently Gasperini *et al.* applied the flexible linker concept with a common molecular semiconductor, 3,6-bis(5-(benzofuran-2-yl)thiophen-2-yl)-2,5-bis(2-ethylhexyl)-2,5-dihydropyrrolo [3,4-*c*]pyrrole-1,4-dione, and prepared the flexibly-linked version: FL-DPP(TBFu)<sub>2</sub> (Scheme 3).<sup>[21b]</sup> OTFTs prepared with pure FL-DPP(TBFu)<sub>2</sub> showed no measurable  $\mu_h$  in contrast to FL-PBTTT, likely due to the higher fraction of insulating alkyl groups. However, as-cast films of the FL-DPP(TBFu)<sub>2</sub> blended with the parent small molecule, DPP(TBFu)<sub>2</sub>, gave interesting results when subject to thermal stress (at 100 °C) for extended time (Fig. 3). The measured  $\mu_h$  was found to decrease by an order of magnitude for the film of pure DPP(TBFu)<sub>2</sub> (0 wt%). However, a considerably smaller decrease is observed when 1 wt% of the FL-DPP(TBFu)<sub>2</sub> was added, and notably at 5 wt%,  $\mu_h$  remained constant. The active layer morphology of these devices, after the extended thermal stress test, showed a drastic difference when adding the FL-DPP(TBFu)<sub>2</sub> (Fig. 3). While the pure DPP(TBFu)<sub>2</sub> (0 wt%) device exhibited small circular domains (*ca.* 100–200 nm) and only a few long crystalline shards, with 1 or 5 wt% of FL-DPP(TBFu)<sub>2</sub> the films exhibited large banded features 200–500 nm in width and more than microns in length. These morphological observations together with the transistor device thermal stability data show clearly that the FL-DPP(TBFu)<sub>2</sub> actively participates in the stabilization of the thin-film charge transport network. Given the polymeric structure of the FL-DPP(TBFu)<sub>2</sub> a plausible explanation for the observed behavior was presented: the FL-DPP(TBFu)<sub>2</sub> was acting as a tie molecule to bridge adjacent crystal domains, effectively locking-in the active layer morphology.

Overall, both strategies of side chain engineering and employing flexible linkers can be powerful tools to tune the morphology of a thin film of a polymer semiconductor in order to gain insights into the factors important for charge transport and also ultimately improve the performance of single-active-component OTFT devices. For other optoelectronic applications, like organic photovoltaics or light emitting diodes, however, two semiconducting components – an electron donor and an electron acceptor – are required.

## 5. Linking Segments for Donor–Acceptor Applications

In the case for organic photovoltaics (OPV), an electron-donating component (typically a p-type conjugated polymer) and an electron-accepting component (most often a small molecule n-type fullerene, but an n-type semiconducting polymer can also be used<sup>[30]</sup>) are blended together and cast into an active layer. The donor and acceptor must be intimately mixed on the length scale of tens of nanometers to afford efficient free charge generation, which is the typical distance that a bound-electron hole pair (an exciton) can diffuse. However, the donor and acceptor components must also be sufficiently de-mixed to allow for the continuous transport of free charges (generated at the donor:acceptor heterojunction) to their respective electrodes. Accordingly, the performance of an OPV is highly dependent on the morphology of this ‘bulk-heterojunction’ (BHJ)<sup>[31]</sup> active layer. In order to gain appreciable control over the degree of phase segregation and the overall BHJ morphology, an understanding of both kinetic and thermodynamic factors of the self-assembly is required.<sup>[32]</sup>

Numerous strategies have been investigated to control the BHJ morphology such as the use of processing additives,<sup>[33]</sup>

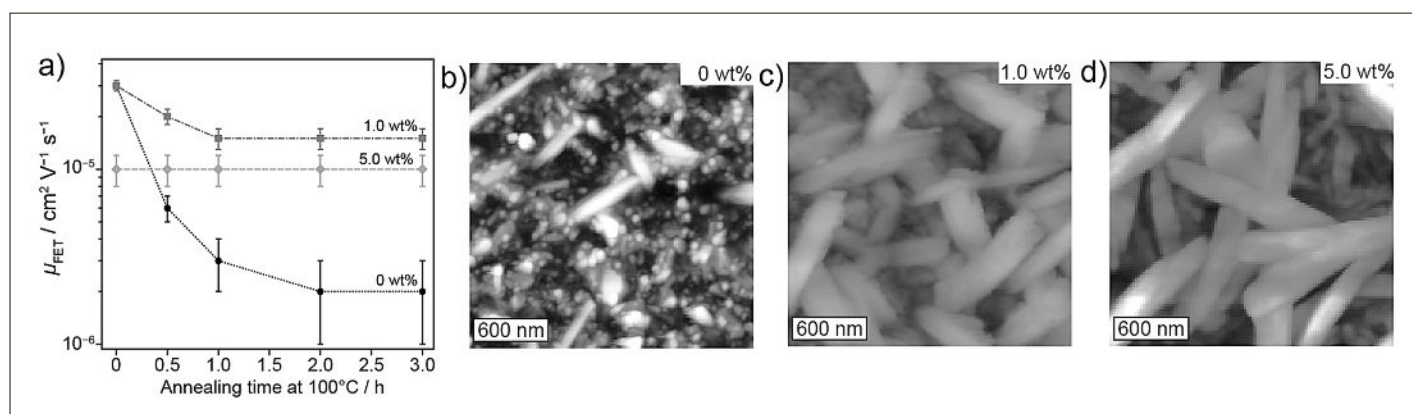


Fig. 3. Thin film transistor performance and morphology of FL-DPP(TBFu)<sub>2</sub>. Panel (a) shows the average extracted field effect mobility as a function of annealing time at 100 °C for transistors of DPP(TBFu)<sub>2</sub> with added FL-DPP(TBFu)<sub>2</sub> at the wt% indicated. Atomic force micrographs (b–d) show the topology of the thin film transistor active layer after 3.0 hours at 100 °C. Adapted from ref. [21b], © 2015 WILEY-VCH Verlag GmbH & Co. KGaA.

and thermal<sup>[34]</sup> or solvent annealing.<sup>[35]</sup> However, these approaches do not change the fundamental limitation of a multicomponent BHJ: the mixed components are kinetically trapped in a metastable morphology given that the thermodynamic equilibrium is separated by domains with a minimum interfacial area (and thus minimal free charge generation).<sup>[36]</sup> While cross-linking<sup>[37]</sup> of the BHJ network triggered by an external stimuli (*e.g.* heat or light) of active functional groups on the ends of the alkyl chains,<sup>[38]</sup> or by using small molecule additives,<sup>[37,39]</sup> can effectively kinetically trap the morphology, this comes at the expense of decrease in performance due to the introduction of charge trapping defects from the crosslinking reactions.<sup>[37a,40]</sup>

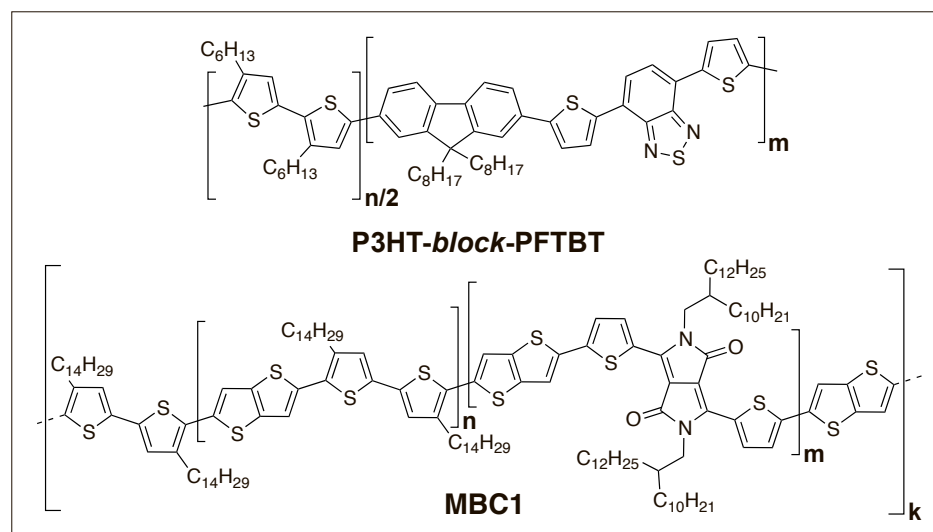
An emerging strategy that has the potential to afford thermodynamically stable morphologies with the ideal donor:acceptor phase separated nanostructures is the use of a donor-*block*-acceptor copolymer in a single-component active layer.<sup>[41]</sup> This prevalent interest stems from the nature of the self-assembling behavior of traditional (non-semiconducting) block copolymers (BCPs), where the incompatibility of the individual blocks drives morphological phase segregation to minimize surface energy while the covalent linkage between the respective blocks prevents macroscopic separation. This concept, applied to semiconducting polymers can afford phase-separated donor:acceptor domains at a size tuned to the length scales for preferential exciton diffusion, while maintaining continuous pathways to enable charge extraction for efficient device performance.<sup>[42]</sup>

Recently, the use of semiconducting BCPs was impressively demonstrated for OPV by Gou *et al.* by using a P3HT-*block*-PFTBT (structure in Scheme 4).<sup>[42b]</sup> Resonant soft X-ray scattering (RSOXS) allowed the authors to illustrate the phase segregation of the blocks at the *ca.* 10 nm length scale (Fig. 4a), giving a reasonable approximation of the ideal BHJ (see schematic in the inset of Fig. 4a). While the champion OPV device prepared with the P3HT-*block*-PFTBT material gave a modest 3% overall solar power conversion efficiency (PCE) under 1 sun conditions (compared to over 10% demonstrated to date with optimized and separate donor and acceptor materials), this demonstration, which establishes benchmark performance for the P3HT-*block*-PFTBT solar cells, nevertheless provides a clear pathway for enhancing efficiencies in fully conjugated block copolymers devices.

One limitation of the P3HT-*block*-PFTBT system is the use of the P3HT block. While its synthesis by the aforementioned quasi-living methods affords facile preparation of all-conjugated block-

copolymers, the non-ideal energy levels and light absorption limit the voltage and current density that can be produced by the device compared to modern optimized low-band gap donor polymers.<sup>[45]</sup> To overcome this limitation, recent reports have pursued methods to obtain BCPs without P3HT, and enabling the use of the common step-growth polycondensation methods in BCP preparation.<sup>[46]</sup> One simple approach to all conjugated BCPs uses di-function-

alized macromonomers (Fig. 4b) to give multi-block copolymers. The clear advantage of this method is that each block can be prepared separately and purified before the final polymerization. However, preparing pure functionalized macromonomers is a major challenge. Recently our group used preparatory size exclusion chromatography to facilitate the preparation of pure macromonomers and obtained an alternating multi-BCP with PBTTT blocks



Scheme 4. All-conjugated block copolymers used for optoelectronic applications.

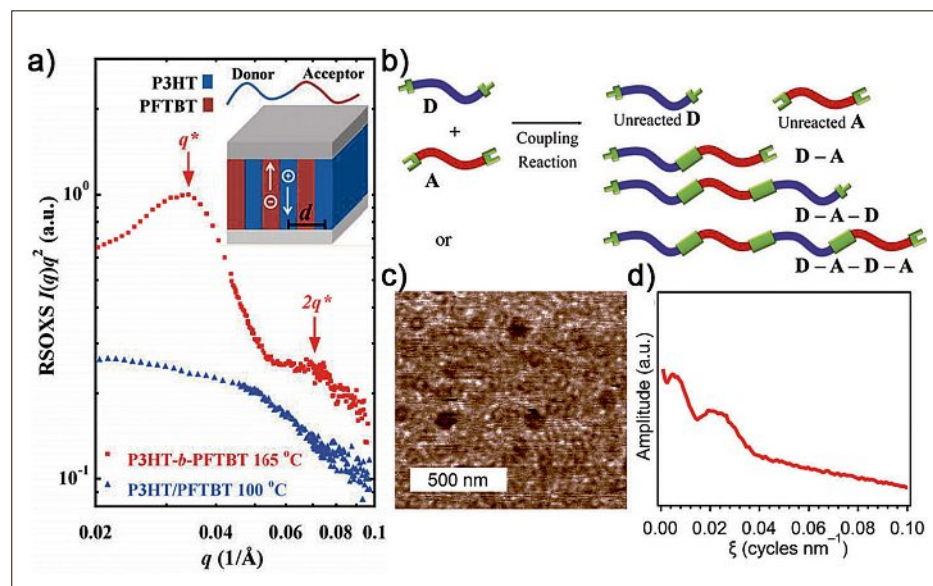


Fig. 4. All conjugated block copolymer approach. (a) Comparison of the morphology in the active layers of optimized P3HT-*b*-PFTBT and P3HT/PFTBT photovoltaic devices using RSOXS. Scattering data are presented as a Kratky plot of  $I(q)q^2$  vs  $q$ , where  $I(q)$  is the scattering intensity and  $q$  is the scattering vector. In optimized P3HT-*b*-PFTBT samples, a well-defined primary peak,  $q^*$  ( $\sim 0.035 \text{ \AA}^{-1}$ ), and second-order reflection,  $2q^*$ , are identified. Schematic illustration of the lamellar morphology is shown in the inset with the average domain spacing indicated as  $d$ . From ref. [42b] used with permission © 2013 American Chemical Society. (b) Scheme for the synthesis of conjugated block copolymers from premade donor and acceptor homopolymers using a coupling reaction. Depending on the degree of end-group control in the homopolymers, products can contain diblock, triblock, and multiblock copolymers as well as unreacted homopolymers. From ref. [43] used with permission © 2015 American Chemical Society. (c) Characterization of the self-assembly of MBC1 showing the phase image from a tapping mode AFM image, and (d) shows the amplitude of the spatial frequency from the FFT of (c). (c) and (d) are adapted from ref. [44]. © The Royal Society of Chemistry 2017.

for the donor and a DPP-based polymer as the acceptor.<sup>[44]</sup> The polymer, coded MBC1 (structure in Scheme 4) with  $n = 14$ ,  $m = 5$  and  $k = 6-8$ , demonstrated nanoscopic phase domain separation visualized by AFM (Fig. 4c) that gave a domain spacing of about 50 nm (Fig. 4d) consistent with the length of PBTBT used (40 nm). Reasonable charge transport across the active layer was observed with a  $\mu_h$  of  $0.08 \text{ cm}^2 \text{ V}^{-1} \text{ s}^{-1}$  (compared to  $9.0 \times 10^{-3} \text{ cm}^2 \text{ V}^{-1} \text{ s}^{-1}$  and  $5.0 \times 10^{-4} \text{ cm}^2 \text{ V}^{-1} \text{ s}^{-1}$ , for the parent donor and acceptor macromonomers). Unfortunately, successful demonstration in OPV devices was not accomplished with MBC1, likely due to the less than ideal energetics of the donor:acceptor combination. However, the successful demonstration of an all-conjugated non-P3HT donor-acceptor block copolymer will open the door for further design of the next generation of semiconducting polymers with thermodynamically stable nanoscopic morphology and properties that are fully tunable by changing the block structure and length. Moreover, understanding how such polymeric structures self-assemble into stable equilibrium morphologies will address the problem of phase segregation as mentioned earlier and allows predictability in processing of such materials into thin films.<sup>[8a,47]</sup> Although, many challenges still remain in developing synthetic approaches for BCPs of a wider range of (macro)monomeric units to yield well defined materials for single-component OPVs at state-of-the-art device efficiencies.<sup>[48]</sup>

## 6. Conclusions and Outlook

Overall, the field of semiconducting polymers has witnessed major developments in the past decades that have resulted in significant improvement in optoelectronic device performance, largely due to the efforts of synthetic chemists in the creation of a vast library of polymers that paves a pathway towards the understanding of the relationship between the solid-state self-assembly (thin film morphology) and the resulting optoelectronic properties. While the complications of grain boundaries, paracrystallinity and, domain connectivity remain as multifaceted problems that frustrate efforts to afford complete control over self-assembly in semiconducting polymers, further efforts in molecular engineering is no doubt the key to fully enabling these material for high-performance devices. It should be noted that the tools of synthetic organic chemistry are also being employed to enhance other aspects of semiconducting polymers, such as the innovation and improvements of conjugated polymer synthesis towards greener synthetic methods,<sup>[49]</sup> or tuning mechani-

cal stability<sup>[50]</sup> of conjugated polymers for truly flexible and wearable devices. Ultimately, to fully appreciate the full potential that conjugated semiconducting polymers possess, an integrative understanding of synthesis, morphological and self-assembly control, processing, and device architecture design will be required.

Received: April 13, 2017

- [1] a) H. Sirringhaus, *Adv. Mater.* **2014**, *26*, 1319; b) L. Dou, J. You, Z. Hong, Z. Xu, G. Li, R. A. Street, Y. Yang, *Adv. Mater.* **2013**, *25*, 6642; c) R. R. Søndergaard, M. Hösel, F. C. Krebs, *J. Polym. Sci., Part B: Polym. Phys.* **2013**, *51*, 16; d) X. Guo, M. Baumgarten, K. Müllen, *Prog. Polym. Sci.* **2013**, *38*, 1832.
- [2] P.-O. Morin, T. Bura, M. Leclerc, *Materials Horizons* **2016**, *3*, 11.
- [3] a) A. Facchetti, *Mater. Today* **2007**, *10*, 28; b) J. E. Anthony, *Nat. Mater.* **2014**, *13*, 773; c) R. A. Street, *Science* **2013**, *341*, 1072.
- [4] a) J. L. Brédas, J. P. Calbert, D. A. da Silva Filho, J. Cornil, *Proc. Natl. Acad. Sci. USA* **2002**, *99*, 5804; b) C.-G. Zhan, J. A. Nichols, D. A. Dixon, *J. Phys. Chem. A* **2003**, *107*, 4184.
- [5] J. E. Northrup, *Phys. Rev. B* **2007**, *76*, 245202.
- [6] K. Okamoto, C. K. Luscombe, *Polym. Chem.* **2011**, *2*, 2424.
- [7] R. J. Kline, M. D. McGehee, E. N. Kadnikova, J. Liu, J. M. J. Fréchet, M. F. Toney, *Macromolecules* **2005**, *38*, 3312.
- [8] a) B. Kuei, E. D. Gomez, *Soft Matter* **2017**, *13*, 49; b) N. Stingelin, *Polym. Int.* **2012**, *61*, 866; c) P. J. Flory, D. Y. Yoon, *Nature* **1978**, *272*, 226.
- [9] F. P. V. Koch, J. Rivnay, S. Foster, C. Müller, J. M. Downing, E. Buchaca-Domingo, P. Westacott, L. Y. Yu, M. J. Yuan, M. Baklar, Z. P. Fei, C. Luscombe, M. A. McLachlan, M. Heeney, G. Rumbles, C. Silva, A. Salleo, J. Nelson, P. Smith, N. Stingelin, *Prog. Polym. Sci.* **2013**, *38*, 1978.
- [10] A. Gasperini, K. Sivula, *Macromolecules* **2013**, *46*, 9349.
- [11] I. McCulloch, M. Heeney, C. Bailey, K. Genevicius, I. MacDonald, M. Shkunov, D. Sparrowe, S. Tierney, R. Wagner, W. Zhang, M. L. Chabiny, R. J. Kline, M. D. McGehee, M. F. Toney, *Nat. Mater.* **2006**, *5*, 328.
- [12] R. Noriega, J. Rivnay, K. Vandewal, F. P. V. Koch, N. Stingelin, P. Smith, M. F. Toney, A. Salleo, *Nat. Mater.* **2013**, *12*, 1038.
- [13] A. Gasperini, X. A. Jeanbourquin, K. Sivula, *J. Polym. Sci., Part B: Polym. Phys.* **2016**, *54*, 2245.
- [14] J. Mei, Z. Bao, *Chem. Mater.* **2014**, *26*, 604.
- [15] Y. Sun, S.-C. Chien, H.-L. Yip, K.-S. Chen, Y. Zhang, J. A. Davies, F.-C. Chen, B. Lin, A. K. Y. Jen, *J. Mater. Chem.* **2012**, *22*, 5587.
- [16] A. Duarte, K.-Y. Pu, B. Liu, G. C. Bazan, *Chem. Mater.* **2011**, *23*, 501.
- [17] C. Kanimozhi, N. Yaacobi-Gross, K. W. Chou, A. Amassian, T. D. Anthopoulos, S. Patil, *J. Am. Chem. Soc.* **2012**, *134*, 16532.
- [18] H. Waters, J. Kettle, S.-W. Chang, C.-J. Su, W.-R. Wu, U. S. Jeng, Y.-C. Tsai, M. Horie, *J. Mater. Chem. A* **2013**, *1*, 7370.
- [19] C. B. Nielsen, E.-H. Sohn, D.-J. Cho, B. C. Schroeder, J. Smith, M. Lee, T. D. Anthopoulos, K. Song, I. McCulloch, *ACS Appl. Mater. Interfaces* **2013**, *5*, 1806.
- [20] J. Yao, C. Yu, Z. Liu, H. Luo, Y. Yang, G. Zhang, D. Zhang, *J. Am. Chem. Soc.* **2016**, *138*, 173.
- [21] a) B. C. Schroeder, Z. Li, M. A. Brady, G. C. Faria, R. S. Ashraf, C. J. Takacs, J. S. Cowart, D. T. Duong, K. H. Chiu, C.-H. Tan, J. T. Cabral, A. Salleo, M. L. Chabiny, J. R. Durrant, I. McCulloch, *Angew. Chem. Int. Ed.* **2014**, *53*, 12870; b) A. Gasperini, X. A. Jeanbourquin, A. Rahmanudin, X. Yu, K. Sivula, *Adv. Mater.* **2015**, *27*, 5541; c) Z. Liang, R. A. Cormier, A. M. Nardes, B. A. Gregg, *Synth. Met.* **2011**, *161*, 1014; d) X. Xiang, W. Shao, L. Liang, X.-Q. Chen, F.-G. Zhao, Z. Lu, W. Wang, J. Li, W.-S. Li, *RSC Adv.* **2016**, *6*, 23300.
- [22] a) L. Ding, H.-B. Li, T. Lei, H.-Z. Ying, R.-B. Wang, Y. Zhou, Z.-M. Su, J. Pei, *Chem. Mater.* **2012**, *24*, 1944; b) X. Zhu, M. C. Traub, D. A. Vanden Bout, K. N. Plunkett, *Macromolecules* **2012**, *45*, 5051; c) X. Lin, M. Hirono, T. Seki, H. Kurata, T. Karatsu, A. Kitamura, D. Kuzuhara, H. Yamada, T. Ohba, A. Saeki, S. Seki, S. Yagai, *Chem. Eur. J.* **2013**, *19*, 6561; d) A. Gasperini, S. Bivaud, K. Sivula, *Chem. Sci.* **2014**, *5*, 4922; e) W. Shao, L. Liang, X. Xiang, H.-j. Li, F.-g. Zhao, W.-s. Li, *Chin. J. Chem.* **2015**, *33*, 847; f) B. C. Schroeder, Y.-C. Chiu, X. Gu, Y. Zhou, J. Xu, J. Lopez, C. Lu, M. F. Toney, Z. Bao, *Adv. Electron. Mater.* **2016**, *2*, 1600104; g) Y. Zhao, X. Zhao, Y. Zang, C.-a. Di, Y. Diao, J. Mei, *Macromolecules* **2015**, *48*, 2048; h) X. Zhao, Y. Zhao, Q. Ge, K. Butrouna, Y. Diao, K. R. Graham, J. Mei, *Macromolecules* **2016**, *49*, 2601; i) Y. Zhao, X. Zhao, M. Roders, A. Gumyusenge, A. L. Ayzner, J. Mei, *Adv. Mater.* **2017**, *29*, 1605056.
- [23] X. Zhang, H. Bronstein, A. J. Kronemeijer, J. Smith, Y. Kim, R. J. Kline, L. J. Richter, T. D. Anthopoulos, H. Sirringhaus, K. Song, M. Heeney, W. Zhang, I. McCulloch, D. M. DeLongchamp, *Nat. Commun.* **2013**, *4*, 2238.
- [24] C. Sciascia, N. Martino, T. Schuettfort, B. Watts, G. Grancini, M. R. Antognazza, M. Zavelani-Rossi, C. R. McNeill, M. Caironi, *Adv. Mater.* **2011**, *23*, 5086.
- [25] A. J. Kronemeijer, E. Gili, M. Shahid, J. Rivnay, A. Salleo, M. Heeney, H. Sirringhaus, *Adv. Mater.* **2012**, *24*, 1558.
- [26] Z. M. Beiley, E. T. Hoke, R. Noriega, J. Dacuña, G. F. Burkhard, J. A. Bartelt, A. Salleo, M. F. Toney, M. D. McGehee, *Adv. Energy Mater.* **2011**, *1*, 954.
- [27] R. Steyrlthner, M. Schubert, I. Howard, B. Klaumünzer, K. Schilling, Z. Chen, P. Saalfrank, F. Laquai, A. Facchetti, D. Neher, *J. Am. Chem. Soc.* **2012**, *134*, 18303.
- [28] W. F. Pasveer, J. Cottaar, C. Tanase, R. Coehoorn, P. A. Bobbert, P. W. M. Blom, D. M. de Leeuw, M. A. J. Michels, *Phys. Rev. Lett.* **2005**, *94*, 206601.
- [29] B. Walker, C. Kim, T.-Q. Nguyen, *Chem. Mater.* **2011**, *23*, 470.
- [30] a) A. Facchetti, *Mater. Today* **2013**, *16*, 123; b) H. Bente, D. Mori, H. Ohkita, S. Ito, *J. Mater. Chem. A* **2016**, *4*, 5340.
- [31] a) S. D. Dimitrov, J. R. Durrant, *Chem. Mater.* **2014**, *26*, 616; b) Y. Tamai, H. Ohkita, H. Bente, S. Ito, *J. Phys. Chem. Lett.* **2015**, *6*, 3417; c) C. J. Brabec, M. Heeney, I. McCulloch, J. Nelson, *Chem. Soc. Rev.* **2011**, *40*, 1185.
- [32] a) A. M. Hiszpanski, P. P. Khlyabich, Y.-L. Loo, *MRS Commun.* **2015**, *5*, 407; b) S. S. Lee, S. Muralidharan, A. R. Woll, M. A. Loth, Z. Li, J. E. Anthony, M. Haataja, Y.-L. Loo, *Chem. Mater.* **2012**, *24*, 2920; c) *Annu. Rev. Chem. Biomol. Eng.* **2010**, *1*, 59.
- [33] a) J. K. Lee, W. L. Ma, C. J. Brabec, J. Yuen, J. S. Moon, J. Y. Kim, K. Lee, G. C. Bazan, A. J. Heeger, *J. Am. Chem. Soc.* **2008**, *130*, 3619; b) N. D. Treat, J. A. Nekuda Malik, O. Reid, L. Yu, C. G. Shuttle, G. Rumbles, C. J. Hawker, M. L. Chabiny, P. Smith, N. Stingelin, *Nat. Mater.* **2013**, *12*, 628.
- [34] E. Verploegen, R. Mondal, C. J. Bettinger, S. Sok, M. F. Toney, Z. Bao, *Adv. Funct. Mater.* **2010**, *20*, 3519.
- [35] a) H. Chen, Y.-C. Hsiao, B. Hu, M. Dadmun, *Adv. Funct. Mater.* **2014**, *24*, 5129; b) J. H. Park, J. S. Kim, J. H. Lee, W. H. Lee, K. Cho,

- J. Phys. Chem. C* **2009**, *113*, 17579; c) A. J. Pearson, T. Wang, R. A. L. Jones, D. G. Lidzey, P. A. Staniec, P. E. Hopkinson, A. M. Donald, *Macromolecules* **2012**, *45*, 1499.
- [36] a) M. Jørgensen, K. Norrman, S. A. Gevorgyan, T. Tromholt, B. Andreasen, F. C. Krebs, *Adv. Mater.* **2012**, *24*, 580; b) I. Fraga Domínguez, A. Distler, L. Lüer, *Adv. Energy Mater.* **2016**, 1601320.
- [37] a) J. W. Rumer, I. McCulloch, *Mater. Today* **2015**, *18*, 425; b) G. Wantz, L. Derue, O. Dautel, A. Rivaton, P. Hudhomme, C. Dagron-Lartigau, *Polym. Int.* **2014**, *63*, 1346.
- [38] a) H. J. Kim, A. R. Han, C.-H. Cho, H. Kang, H.-H. Cho, M. Y. Lee, J. M. J. Fréchet, J. H. Oh, B. J. Kim, *Chem. Mater.* **2012**, *24*, 215; b) J. E. Carle, B. Andreasen, T. Tromholt, M. V. Madsen, K. Norrman, M. Jørgensen, F. C. Krebs, *J. Mater. Chem.* **2012**, *22*, 24417; c) Y.-J. Cheng, C.-H. Hsieh, P.-J. Li, C.-S. Hsu, *Adv. Funct. Mater.* **2011**, *21*, 1723; d) S. Miyanishi, K. Tajima, K. Hashimoto, *Macromolecules* **2009**, *42*, 1610.
- [39] B. Liu, R.-Q. Png, L.-H. Zhao, L.-L. Chua, R. H. Friend, P. K. H. Ho, *Nat. Commun.* **2012**, *3*, 1321.
- [40] a) V. I. Madogni, B. Kounouhéwa, A. Akpo, M. Agbomahéna, S. A. Hounkpatin, C. N. Awanou, *Chem. Phys. Lett.* **2015**, *640*, 201; b) T. Heumueller, W. R. Mateker, A. Distler, U. F. Fritze, R. Cheacharoen, W. H. Nguyen, M. Biele, M. Salvador, M. von Delius, H.-J. Egelhaaf, M. D. McGehee, C. J. Brabec, *Energy Environ. Sci.* **2016**, *9*, 247; c) F. Fungura, W. R. Lindemann, J. Shinar, R. Shinar, *Adv. Energy Mater.* **2016**, 1601420.
- [41] S. B. Darling, *Energy Environ. Sci.* **2009**, *2*, 1266.
- [42] a) F. Lombeck, H. Komber, A. Sepe, R. H. Friend, M. Sommer, *Macromolecules* **2015**, *48*, 7851; b) C. Guo, Y.-H. Lin, M. D. Witman, K. A. Smith, C. Wang, A. Hexemer, J. Strzalka, E. D. Gomez, R. Verduzco, *Nano Letters* **2013**, *13*, 2957.
- [43] Y. Lee, E. D. Gomez, *Macromolecules* **2015**, *48*, 7385.
- [44] A. Gasperini, M. Johnson, X. Jeanbourquin, L. Yao, A. Rahmanudin, N. Guijarro, K. Sivula, *Polym. Chem.* **2017**, *8*, 824.
- [45] a) S.-Y. Ku, M. A. Brady, N. D. Treat, J. E. Cochran, M. J. Robb, E. J. Kramer, M. L. Chabiny, C. J. Hawker, *J. Am. Chem. Soc.* **2012**, *134*, 16040; b) M. Sommer, H. Komber, S. Huettner, R. Mulherin, P. Kohn, N. C. Greenham, W. T. S. Huck, *Macromolecules* **2012**, *45*, 4142; c) K. A. Smith, Y.-H. Lin, J. W. Mok, K. G. Yager, J. Strzalka, W. Nie, A. D. Mohite, R. Verduzco, *Macromolecules* **2015**, *48*, 8346.
- [46] a) J. W. Mok, D. Kipp, L. R. Hasbun, A. Dolocan, J. Strzalka, V. Ganesan, R. Verduzco, *J. Mater. Chem. A* **2016**, *4*, 14804; b) D. Gao, G. L. Gibson, J. Hollinger, P. Li, D. S. Seferos, *Polym. Chem.* **2015**, *6*, 3353.
- [47] D. Kipp, J. Mok, J. Strzalka, S. B. Darling, V. Ganesan, R. Verduzco, *ACS Macro Lett.* **2015**, *4*, 867.
- [48] a) T. Yokozawa, Y. Ohta, *Chem. Rev.* **2016**, *116*, 1950; b) R. Grisorio, G. P. Suranna, *Polym. Chem.* **2015**, *6*, 7781; c) V. Senkovskyy, R. Tkachov, H. Komber, M. Sommer, M. Heuken, B. Voit, W. T. S. Huck, V. Kataev, A. Petr, A. Kiriy, *J. Am. Chem. Soc.* **2011**, *133*, 19966; d) J. Wang, T. Higashihara, *Polym. Chem.* **2013**, *4*, 5518.
- [49] a) T. P. Osedach, T. L. Andrew, V. Bulovic, *Energy Environ. Sci.* **2013**, *6*, 711; b) A. Marrocchi, A. Facchetti, D. Lanari, C. Petrucci, L. Vaccaro, *Energy Environ. Sci.* **2016**, *9*, 763.
- [50] S. Savagatrup, A. D. Printz, T. F. O'Connor, A. V. Zaretski, D. Rodriguez, E. J. Sawyer, K. M. Rajan, R. I. Acosta, S. E. Root, D. J. Lipomi, *Energy Environ. Sci.* **2015**, *8*, 55.